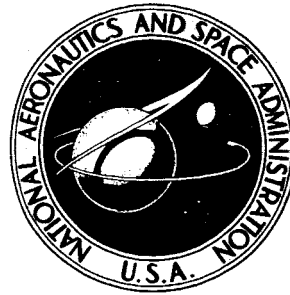


**NASA TECHNICAL  
MEMORANDUM**



**NASA TM X-1506**

**NASA TM X-1506**

FACILITY FORM 602	_____ (ACCESSION NUMBER)	_____ (THRU)
	_____ (PAGES)	_____ (CODE)
	_____ (NASA CR OR TMX OR AD NUMBER)	_____ (CATEGORY)

**A 4500° R (2500° K)  
FLOWING-GAS FACILITY**

*by Jack G. Slaby, Byron L. Siegel,  
William F. Mattson, and William L. Maag*

*Lewis Research Center  
Cleveland, Ohio*

A 4500<sup>o</sup> R (2500<sup>o</sup> K) FLOWING-GAS FACILITY

By Jack G. Slaby, Byron L. Siegel, William F. Mattson,  
and William L. Maag

Lewis Research Center  
Cleveland, Ohio

NATIONAL AERONAUTICS AND SPACE ADMINISTRATION

---

For sale by the Clearinghouse for Federal Scientific and Technical Information  
Springfield, Virginia 22151 - CFSTI price \$3.00

# A 4500° R (2500° K) FLOWING-GAS FACILITY

by Jack G. Slaby, Byron L. Siegel, William F. Mattson, and William L. Maag

Lewis Research Center

## SUMMARY

The design and operation of a high-temperature flowing-gas heater is described. The heater consists of four identical heater stages, each individually controlled. The heating elements consist of flat tungsten plates which are electrically resistance heated by high direct-current power supplies and operate at surface temperatures above 5000° R (2780° K). The maximum power that can be transferred to the gas is about 1.5 megawatts.

The gas flows through the four heater stages in series. Gas temperatures exceeding 4500° R (2500° K) have been obtained with hydrogen, helium, and nitrogen. Operating life of the heater elements is 10 hours or more. Heater elements and associated components are easy to fabricate and assemble. Heater development areas that are discussed include power supply selection, connection of high current busing to the heater, heater expansion at operating temperature, materials compatibility, and heater surface temperature profiles associated with the physical dimensions of the heater.

## INTRODUCTION

Reactor fuel-element designs can be partly evaluated out-of-pile by heating the elements to operating temperature with a flowing hot gas. The effect of aerodynamic forces on the fuel elements and support structure as well as pressure drop characteristics can thereby be determined. An operational hot gas facility has accordingly been developed at the Lewis Research Center for the purpose of conducting high-temperature fuel-element research. The results of some experiments using this facility are reported in reference 1.

This report describes the operational hot gas facility with flat tungsten plates as the heating elements. Flat tungsten plates were first used to simulate nuclear heating by electric heating, as described in reference 2, because they were easy to heat electrically and easy to fabricate. The tests of reference 2, which were predominantly heat-transfer

tests, demonstrated that thin tungsten plates could be successfully operated at surface temperatures of  $5000^{\circ}\text{R}$  ( $2780^{\circ}\text{K}$ ).

Therefore, with the experience gained in the initial heat-transfer and fuel-element work on flat plates, a heater was constructed that is capable of heating hydrogen, helium, and nitrogen to outlet gas temperatures of  $4500^{\circ}\text{R}$  ( $2500^{\circ}\text{K}$ ).

The following areas associated with the heater development are discussed:

- (1) Selection of a power supply for the heating element
- (2) Provisions for conducting large electrical currents to the heater, yet allowing for heater expansion
- (3) Selection of compatible heater and heater housing materials
- (4) Operating goals of the heater in terms of operational life, temperature level, and gases used
- (5) Heater surface temperature profiles, both calculated and experimental, associated with the physical dimensions of the heater

A table is included that lists the operating conditions for the various gases used.

## FACILITY DESCRIPTION

The gas heater facility is shown photographically in figure 1 and schematically in figure 2. The important components shown in these figures include

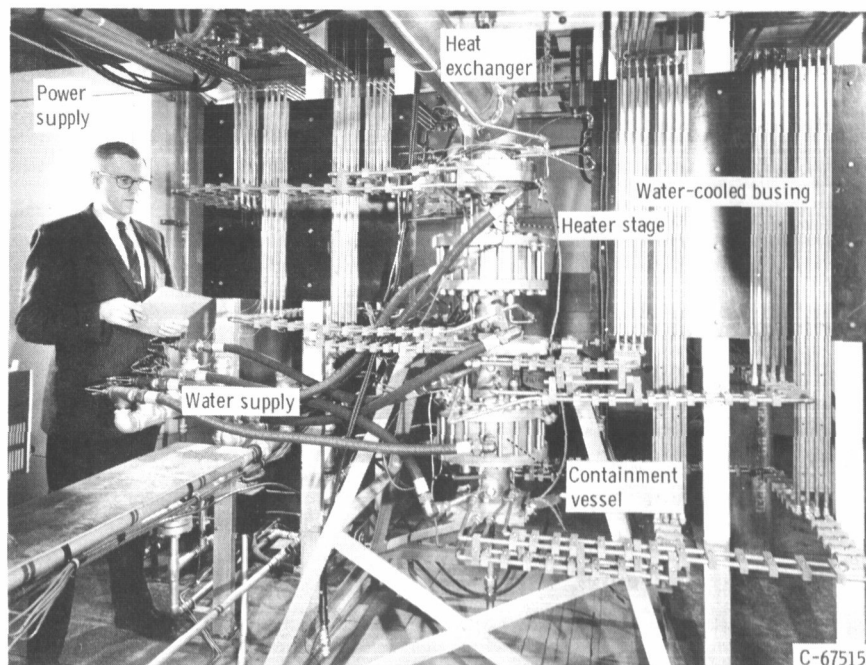


Figure 1. - Four-stage flat-plate gas-heater facility.

- (1) Four heater stages, each stage consisting of five tungsten flat plates in a boron nitride housing
- (2) Four individually controlled direct-current power supplies, one for each heater stage
- (3) Water-cooled electrical busing, some of which serve as electrode tension springs to accommodate heater expansion
- (4) A heat exchanger to cool the gas before exhausting through piping to the atmosphere
- (5) Two water flow systems, one for electrical busing and the other for cooling the heat exchanger and water-jacketed containment vessels
- (6) A gas flow system

A more detailed description of the individual components is given under the appropriate subheadings; however, certain components such as the power supply and heating elements are discussed further in the section OPERATIONAL CHARACTERISTICS.

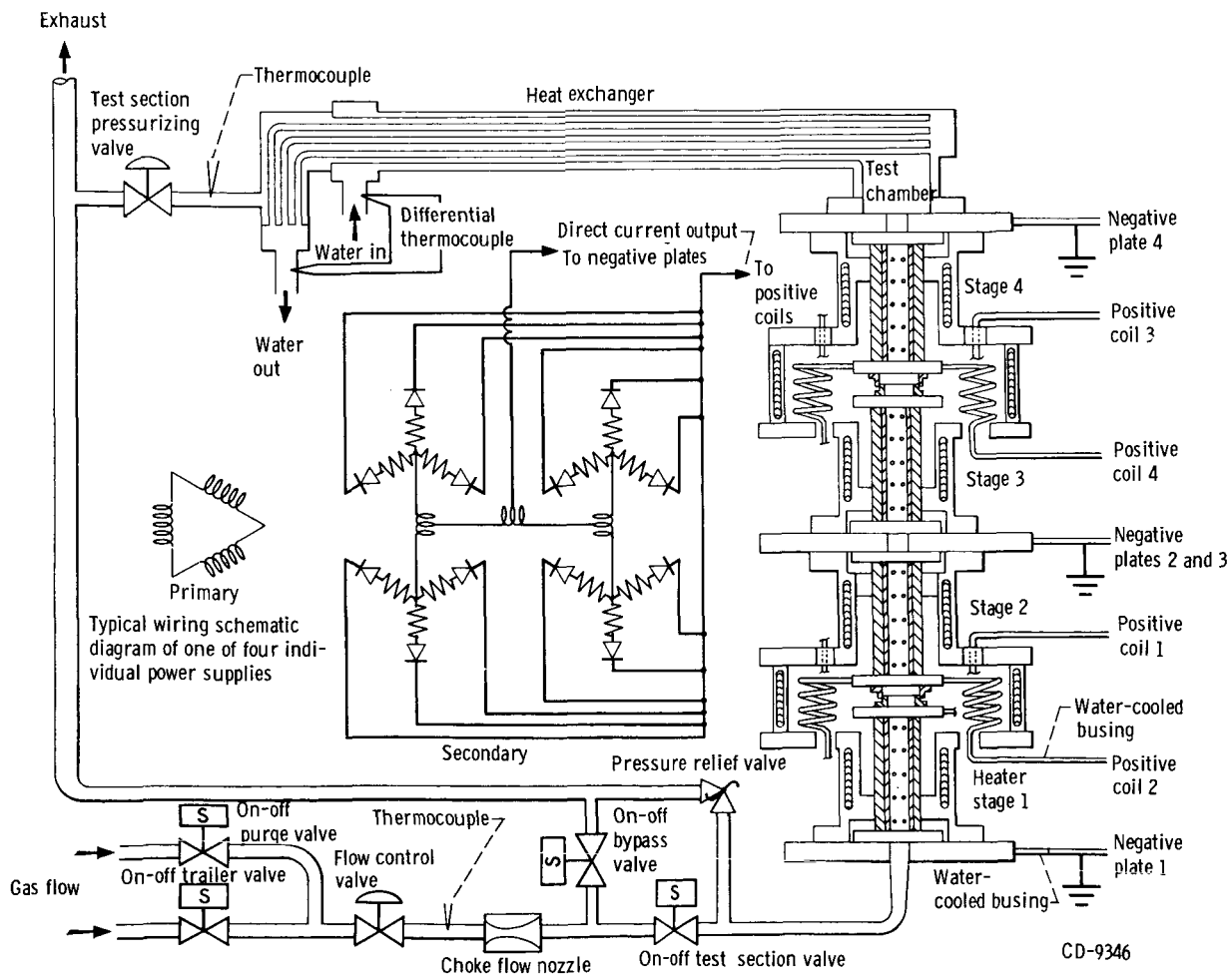


Figure 2. - Schematic diagram of power supply, heater stages, electrical busing, and gas and water flow systems.

## Heater Assembly

The heater consists of four identical heating stages in series through which the gas flows. Each stage is electrically heated by one of the four power supplies. The heating elements consist of five flat tungsten plates made from rolled tungsten sheet 0.030 inch (0.762 mm) thick. Each plate is ground into a shape, as shown in figure 3. The tabs on each end serve as bus connections and permit the gas to flow unimpeded through the plates which are assembled for parallel current flow. Plate spacing is maintained by groups of cylindrical tungsten spacers, as shown in figure 4. Each group of four spacers is placed over holes disintegrated in the tungsten plates. The assembly of five plates with spacers is held together with tungsten bolts and nuts. Fifteen pairs of spacer assemblies are necessary to support the five plates against the electromagnetic and aerodynamic forces to which they are subjected at maximum operating conditions. The assembled plates are clamped onto buses that provide the current path into and out of the elements. In general, each heater element is rigidly bused to a water-cooled copper plate on one end and a water-cooled electrode tension spring on the other end. The rigid copper plate always serves as the electrical ground or negative power connection, as shown schematically in figure 5. Figure 3 shows the heater elements surrounded by a boron nitride insulating housing. The housing forms a 1- by 1/2-inch (2.54- by 1.27-cm) flow duct through which gas flows between the plates. The boron nitride housing consists of two inner halves 1 1/2 inch (3.81 cm) in outside diameter held together by a hollow cylin-

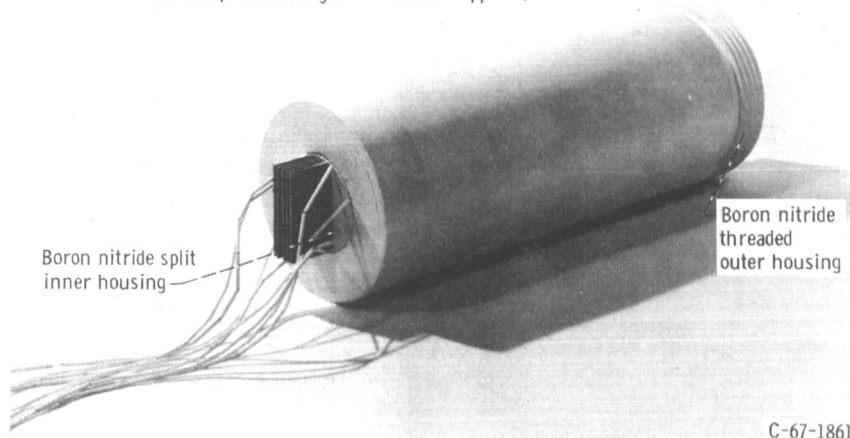
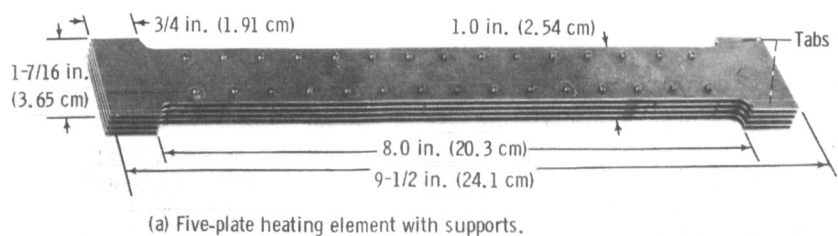
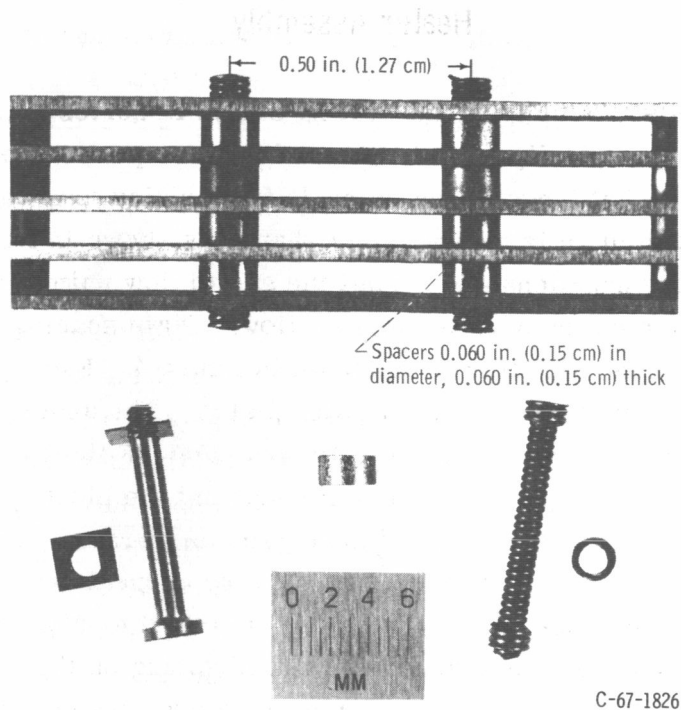
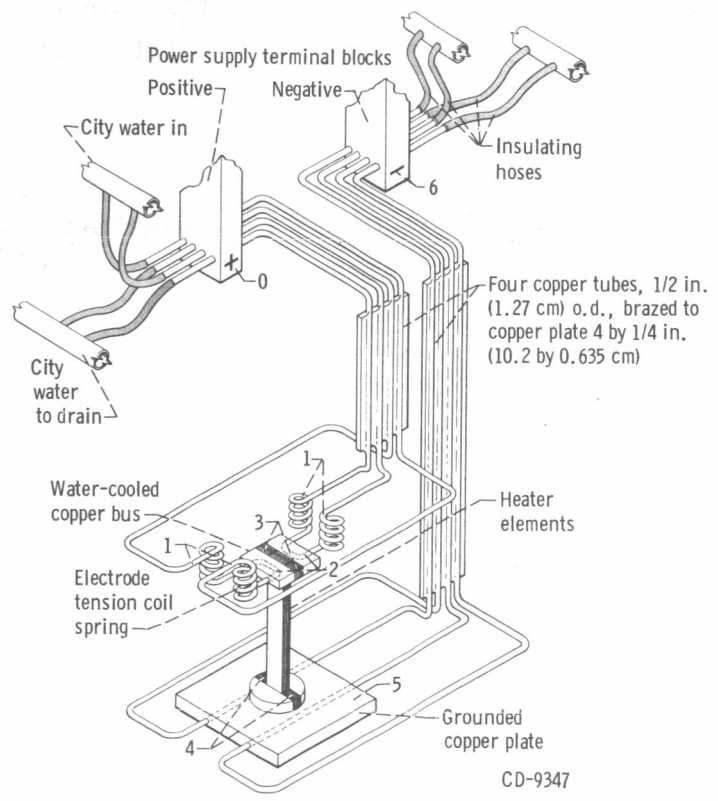


Figure 3. - One heater stage of four-stage flat-plate heater.



C-67-1826

Figure 4. - Section of heater plates with spacers and two types of nuts and bolts.



CD-9347

Figure 5. - Schematic arrangement of water-cooled busing. (Voltage drop location indicated by numbers 0 to 6.)

drical piece 3 inches (7.62 cm) in diameter. This outer cylinder is threaded on one end and screwed into the pressure vessel housing to prevent bypass of the gas around the heater elements. The prevention of bypass is extremely important because all the flow must pass over the heater elements in order to achieve a high outlet gas temperature. Thus, the plates are uniformly cooled, and the possibility of hot spotting is reduced (as experienced in mesh heaters ref. 3).

The exit of the first stage (fig. 2) is connected to the inlet of the second stage by an electrical insulating boron nitride duct which permits relative expansion between the two stages. This same flow arrangement is used at the exit of the third stage and the inlet of the fourth stage. In addition, the fixed ends of the second and third stages are fastened to a common water-cooled copper plate. The water cooling permits large electrical currents to be carried in the small copper tubing. The copper tubing from the negative bus terminates at the copper electrical ground plate. The heated gas flows through a rectangular hole in the center of the plate. Tungsten insulating shields line the periphery of this rectangular hole to protect the copper from the hot gases and to minimize the heat loss to the copper plate. Similar tungsten insulating shields are added to the rectangular hole in the exit plate between the fourth stage and the heat exchanger. A schematic diagram of the flow system, power supply, heater, and associated components as used in this facility is shown in figure 2.

## Power Supply

The electrical power source for the heaters consists of four identical low voltage direct-current power supplies. These power supplies were to be compatible with heater resistances of about 2 milliohms. The important specifications for the four identical power supplies are as follows:

Input: 2400 volts, 3 phases, 230 amperes (ac)

Output: 36 volts, 15 000 amperes (dc), 12-phase dc rectification, continuous operation with a minimum overload rating of 18 750 amperes for 2 hours at 36 volts (dc)

Control: Variable voltage saturable reactor control. The output voltage is adjustable from 10 to 100 percent of rated voltage at 1 to 100 percent of rated power.

Alternating-current ripple voltage: The ratio of effective (rms) value of ripple voltage to the average value of the total output direct-current voltage is less than 10 percent when connected to a resistive load and operating at any point in the voltage range of 30 to 100 percent of rated voltage.

Power supply flexibility: The power supplies have been constructed for parallel and series operation in addition to the normal individual operation. The changeover to either series, parallel, or series-parallel operation, however, does require a con-



siderable amount of control modification. The following continuous duty ranges are

Current, A	Voltage, V(dc)
15 000	at 0 to 144
30 000	at 0 to 72
60 000	at 0 to 36

## Gas Flow System

Hydrogen, nitrogen, or helium was supplied to the flow system from tube trailers at a maximum pressure of 2400 psi ( $16.5 \times 10^6$  N/m<sup>2</sup>). The gas then flowed from the trailer through a remotely operated control valve, a choked flow nozzle, and an on-off valve that supplied gas directly to the heater. The gas flow was metered by the choked flow nozzle. A constant mass flow through the test section was assured as long as a choked condition was maintained in the nozzle for a constant upstream density. Three different size nozzles were available to cover a wide range of gas flow rates. Typical flow rates are listed in table I. From the heater, the hot gas flowed through a water-cooled test section and into a single-pass gas-to-water tube-and-shell heat exchanger where it was cooled below 1500° R (835° K) before being exhausted to the atmosphere. Downstream of the heat exchanger is a remotely operated back pressure valve whose purpose is twofold. Prior to operation the valve is closed to check the system for gas leaks; during operation the valve is used to vary the pressure level in the test section.

For safety reasons, before using hydrogen for the test gas, the entire gas flow system is purged with nitrogen. The controls were set for fail-safe operation so that if any preset safety permissive stops the hydrogen flow, nitrogen would automatically purge the system. In such a case, the electrical power to the heater would also be automatically shut down. A heater bypass line with a pressure relief valve was also incorporated to prevent accidental overpressuring of the heat exchanger.

## Water Flow Systems

There are two water flow systems associated with this facility. Cooling tower water was used to cool the containment vessel, flanges, and heat exchanger. City water was used to cool the electrical busing in order to avoid the impurities normally present in cooling tower water. These impurities might affect either the boiling burnout limit or conduct current and generate heat. Figure 5 shows a typical flow schematic of the water-

cooled electrical busing between the positive and negative power supply terminal blocks and the heater elements. (Part of the water-cooled busing is also shown in fig. 1.) These bus plates have the appearance of manometer boards. Each of these bus plates consists of four 1/2-inch- (1.27-cm-) diameter copper tubes furnace brazed to 1/4-inch- (6.35-cm-) thick copper plates to minimize internal power generation within the tubing. The water flow path through the busing, shown schematically in figure 5, can be considered to start at the positive terminal block of the power supply. The water flows from the terminal block through a 1/2-inch- (1.27-cm-) diameter copper tube into one of the tubes brazed to the 1/4-inch- (0.635-cm-) thick copper plate. The water continues through an electrode tension spring into the water-cooled copper bus to which one end of the heater element is clamped. The water returning to the power supply terminal block follows a similar flow path only in reverse order. The water flow path from the power-supply negative terminal block is identical to that of the positive terminal block with the exception that the water flows through a copper electrical ground plate instead of the electrode tension springs and water-cooled copper bus. There are two parallel water flow paths which account for the two supply and two return lines shown in each terminal block (four 1/2-inch- (1.27-cm-) diameter copper tubes). The four heaters are electrically grounded through a common lead attached to the three copper plates shown in figure 2. The water supply lines are electrically isolated from the power-supply buses by rubber hoses.

A pump capable of an outlet pressure of 125 psi ( $8.6 \times 10^5 \text{ N/m}^2$ ) is used to supply water at a flow rate of 4 gallons per minute ( $2.52 \times 10^{-4} \text{ m}^3/\text{sec}$ ) through each heater electrode. Each of the parallel water flow loops supplying power to the heater has a hand valve for adjusting water flow rate through a flowmeter located on the return side of the busing. A water flow switch also located on the return side of each flow loop shuts down the power supplies in the event of an electrode failure.

In the heat exchanger, the water flow is two-pass: It first flows through the annulus surrounding the shell, and into a plenum. From the plenum, it returns through the tubes.

## Instrumentation

The instrumentation used is shown in the flow schematic diagram in figure 2. The current flowing through each stage of the heater was measured by a calibrated shunt with a 1-millivolt voltage drop per 400 amperes. The axial voltage drop along the heater plates was measured either by attaching voltage tap wires under the spring nuts, which clamp the heater plates and spacers together, or by placing the voltage tap wires into holes disintegrated into the edges of the plates, as described in reference 2. The nuts, plates, and spacers are shown in figure 4. Eight voltage taps were attached at different axial locations to each of the four sets of heater plates, thus giving voltage profiles for each stage. These

voltages were measured and printed out on a digital voltmeter.

For some tests, it was unnecessary to know the incremental axial voltage drop. In these instances, it was convenient to measure only the voltage drop across the entire stage length. For ease of attachment, voltage taps were thus connected to the water-cooled copper bus on one end of the heater plates and to the water-cooled copper plate at the opposite end. The voltage drop across these attachment points (entire stage length) included that due to clamping contact resistance. This portion of the voltage drop (which is actually a small portion of the voltage drop across the attachment points) was then calibrated as a function of current through the test section. The true test section voltage drop was obtained by subtracting the contact drop from the measured total stage voltage drop.

The gas temperature leaving the heater could be measured with a shielded thermocouple. However, space limitation and the lack of a reliable high-temperature thermocouple required that another means be used to determine the heater gas temperature. The gas temperature was calculated from a heat balance on the heat exchanger. The heat exchanger water flow rate was measured with a calibrated orifice and the water temperature rise with a differential iron-constantan thermocouple. Water temperatures either to the electrodes or the containment vessel were measured by type K thermocouples (ref. 4).

All water flow rates to electrodes and the containment vessel were individually measured by rotometers. A choked flow nozzle was used to measure the gas flow rate, which was set by adjusting the nozzle inlet pressure at room temperature. Constant gas flow was maintained providing the exit pressure was not raised sufficiently to unchoke the nozzle. The heater-inlet, heater-outlet, and nozzle-inlet static pressures were measured by temperature compensated strain-gage-bridge pressure transducers. All pressures, temperatures, and currents were continuously recorded on null-balance potentiometer-type recorders.

## Method of Calculation

The heater exit gas temperature  $T_1$  was calculated from a heat balance on the heat exchanger. This calculation was possible because the outlet gas temperature from the heater did not drop a significant amount before entering the heat exchanger. Thus

$$\bar{W}c_{p_g} (T_1 - T_2) = W_1 c_{p_w} \Delta T_1$$

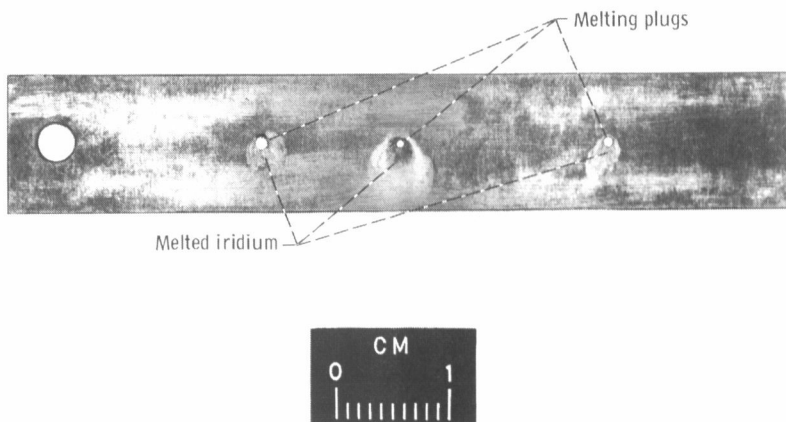
$$T_1 = \frac{W_1 c_{p_w} \Delta T_1}{W \bar{c}_{p_g}} + T_2$$

The symbols are defined in appendix A, and  $W$ ,  $W_1$ ,  $\Delta T_1$ , and  $T_2$  were measured values. The gas properties used were taken from references 5 and 6. The outlet gas temperature  $T_1$  was verified by melting plugs of silver, platinum, rhodium, and iridium. Figure 6 is a typical photograph after a test run showing three iridium melting plugs mounted into holes on a tungsten plate at the heater exit. Prior to running the test, the plugs were peened flush with the tungsten plate surface. The calculated temperature was  $4950^\circ \text{R}$  ( $2750^\circ \text{K}$ ), whereas the actual melting point of iridium is  $4910^\circ \text{R}$  ( $2730^\circ \text{K}$ ). Data from this run (run 3) are tabulated in table I.

The temperature profile along the heater length was obtained in the following manner: Incremental voltage readings  $\Delta V$  were recorded along the length of the heater  $\Delta L$ . The current  $I$  through the heater cross-sectional area  $A$  was measured. The resistivity was calculated by

$$\zeta = \frac{\Delta V}{I} \frac{A}{\Delta L}$$

The incremental heater surface temperature was determined from a plot of resistivity against temperature, as given in reference 7.



C-67-1275-A

Figure 6. - Iridium melting plugs mounted in tungsten plate.

## OPERATIONAL CHARACTERISTICS

The selection of the power supply and the electrical-mechanical considerations associated with delivering high amperage to a heating element are discussed in this section. Also discussed are the selection of heater and heater housing materials, the goals of the heater (in terms of operational life, temperature levels, and gases used) and the temperature profiles (both calculated and experimental) associated with the physical dimensions of the heater.

### Power Supply Selection

The power supply was selected to be compatible with the resistivity of a heater-element consisting of flat tungsten plates electrically connected in parallel. With this type of heating element, the cold heater resistance is extremely low. For example, one heater stage has a room-temperature resistance of about 120 microhms. Even at a temperature of  $5000^{\circ}\text{R}$  ( $2780^{\circ}\text{K}$ ), where the resistance increased by a factor of 15, the heater resistance is less than 2 milliohms. With such a low resistance load at startup, a large transient inrush current would produce electromagnetic forces which could damage the heating elements or instrumentation unless the plates are well supported.

Previous experience on a single-phase alternating-current saturable-reactor-controlled power supply, described in reference 2, resulted in measured transient currents of over 100 000 amperes when connected to a similar flat plate heating element. Since single-phase alternating-current voltage varies with time, over a range from zero to a maximum value, the current surge is dependent on the voltage value in existence at the time the circuit is energized. Fortunately polyphase rectification reduces this effect because, for a given average voltage, the maximum ripple direct-current voltage is less than the maximum single-phase alternating-current voltage. Another important feature of the power supply is the ability to open the alternating-current supply to the magnetic amplifier control circuit at startup. Thus, maximum internal impedance is in the circuit at startup, which further reduces the current surge.

Rectification does not produce true direct-current voltage. Direct-current output voltages and currents contain superimposed ripples. The magnitude of these ripples or harmonics depends on the reactance of the circuit. The harmonic frequencies are dependent on the input supply frequency and the number of rectified phases. A single-line diagram of one power supply is shown in the schematic drawing of figure 2. Polyphase rectification (12 phases in these power supplies) reduces the ripple voltage. The ripple frequency of these power supplies is 720 cps (720 Hz). Generally, the higher the ripple frequency, the lower the ripple voltage.

Automatic voltage or constant voltage control was specified because the resistance of the heating element increases with temperature. With this specification, the presence of a hot spot would increase the resistance and decrease the current flow tending to stabilize operation at a slightly higher temperature. The selection of constant current control, however, would increase power generation and tend toward unstable operation.

## High-Current Water-Cooled Busing

The power supply ratings (36 V, 15 000 A dc at continuous duty) were chosen to match the electrical resistance of the heating elements. A nominal current rating for uncooled copper busing is about 1000 amperes per square inch ( $155 \text{ A/cm}^2$ ) of cross-sectional current area. Thus, approximately 16 square inches ( $103 \text{ cm}^2$ ) of copper are required for each positive and each negative bus at the power supply. Terminating the buses of the power supplies into a compact heater imposes a physical size limitation that necessitates the use of water-cooled busing. Decreasing the busing size by water cooling provided a means to incorporate heater-element expansion into the busing design as discussed in the section Heater Expansion. In addition, the smaller busing at the test section provided more available space and permitted flexibility in instrumentation design and heater-element replacement. The penalty associated with small water-cooled buses is the large voltage drop which reduces the voltage available for the heater itself.

Voltage drop across busing. - Figure 5 is a schematic presentation of the various locations and notation of the voltage drops associated with the water-cooled busing. The voltage available at the heater  $V_{3-4}$  is equal to the power-supply voltage  $V_{0-6}$  less any voltage drops associated with busing to and from the heater. These voltage drops or losses consist of three parts:

- (1) The voltage drop from the power supply to and from the containment vessel designated as  $V_{0-1}$  and  $V_{5-6}$
- (2) The voltage drop inside the containment vessel associated with the drop across the electrode tension springs designated as  $V_{1-2}$
- (3) The voltage drop due to contact resistance between the clamping of the heating elements to the copper or molybdenum buses and plates designated as  $V_{2-3}$  and  $V_{4-5}$

The following section shows that, although each power supply is rated at 540 kilowatts, the most power that can be transferred to the gas, in view of the abovementioned voltage losses, is about 375 kilowatts, or a total of 1.5 megawatts for all four power supplies under the most favorable circumstances. Consider first the voltage losses to and from the power supply external to the containment vessel.

Busing drop external to containment vessel: As described in the FACILITY DESCRIPTION section, the busing from each power supply to the heater containment vessel consisted of a negative and a positive bus. A schematic drawing of the busing arrangement is shown in figure 5; figure 1 shows only a part of the busing. Buses consist of water-cooled tubes brazed to copper plates over most of the length between the terminal block and the test section. In order to facilitate connection at the containment vessel, only the copper water-cooled tubes were continued to the containment vessel. The copper tubes were supported by electrical insulating support clamps in the region where the tubes are not brazed to the copper bus plate. The water-cooled copper plate is 4 by 1/4 inch (10.2 by 0.635 cm) in cross-sectional area and the four copper tubes brazed to the plate are each 1/2 inch (1.27 cm) in outside diameter.

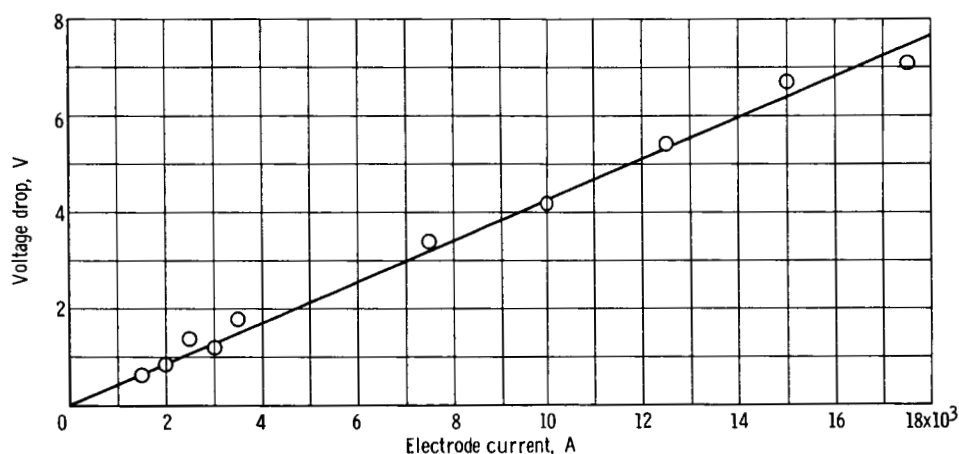


Figure 7. - Voltage drop across electrodes external to containment vessel as function of electrode current.

Figure 7 shows the voltage drop across the water-cooled busing outside the containment vessel as a function of power supply current. As shown in figure 5 this voltage drop includes both positive  $V_{0-1}$  and negative  $V_{5-6}$  drops. As an example, at the maximum continuous duty current value of 15 000 amperes, the sum of  $V_{0-1}$  and  $V_{5-6}$  is 6.4 volts.

Electrode tension spring drop: One end of each heating element is rigidly fixed to a water-cooled copper plate. This plate serves as the electrical ground or negative bus connection between the four 1/2-inch- (1.27-cm-) diameter water-cooled tubes external to the containment vessel and the heating elements. The other end of the heater is clamped to a water-cooled copper bus. Attached to the copper bus are four water-cooled electrode tension springs. These springs are shown photographically in figure 8 and schematically in figure 5.

The purpose of tension in the electrode tension springs is discussed in the Heater Expansion section. The four 5/16-inch- (0.79-cm-) diameter electrode tension springs

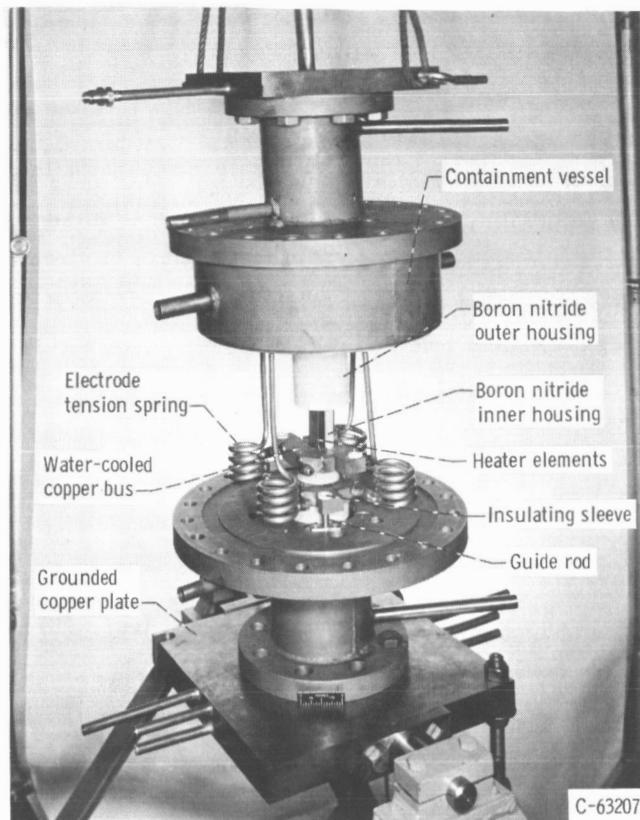


Figure 8. - Two heater stages during assembly.

are connected to the four 1/2-inch- (1.27-cm-) diameter copper water-cooled tubes located outside the containment vessel. Each of the four electrode tension springs is electrically and mechanically connected in parallel. At the maximum continuous duty current of 15 000 amperes, each spring carries 3750 amperes. The voltage drop across the electrode tension springs is shown as a function of current in figure 9. As an example, at 15 000 amperes through the heater, the electrode tension spring voltage drop  $V_{12}$  is 3.2 volts.

**Contact resistance drop:** The contact resistance voltage drops are relatively small. The drop  $V_{2-3}$  is associated with the clamping between the water-cooled copper bus and the heating-element tabs. The drop  $V_{4-5}$  is associated with both the clamping between the molybdenum bus and the heating-element tabs, and between the molybdenum bus and the copper electrical ground plate. As an example, at 15 000 amperes, the summation of  $V_{2-3}$  and  $V_{4-5}$  is less than 0.3 volt.

In summary, the total voltage drop (external busing, 6.4 V; electrode tension springs, 3.2 V; and contact resistance, 0.3 V) at 15 000 amperes is slightly less than 10 volts. Thus at maximum power, the voltage available at the heater is about 26 volts. Consequently, whenever large amperage power supplies are considered, either large buses



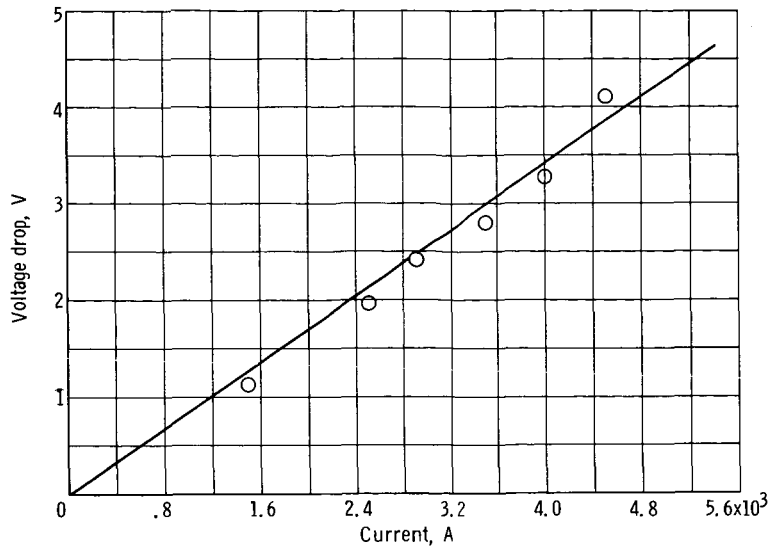


Figure 9. - Voltage drop across electrode tension spring as function of current through spring. Electrode spring outside diameter, 5/16 inch (0.794 cm); copper wall thickness, 1/32 inch (0.079 cm); number of turns per spring, four; outside diameter of spring, 2 $\frac{1}{8}$  inch (5.40 cm).

must be used at the expense of available space and flexibility, or a power loss penalty must be accepted as the convenience of water cooling.

Heater expansion. - The electrode tension springs were designed to accommodate expansion of the heater element at operating temperature without exerting too great a force on the element to cause excessive creep. A predetermined tension force was applied to the electrode tension spring during assembly so that, at maximum operating temperature, tension existed on the heating elements. The tension prevented buckling of the heater plates and subsequent flow blockage. Each tension spring was fabricated from 5/16-inch- (0.79-cm-) diameter copper tubing with 1/32-inch- (0.079-cm-) thick wall and formed into a four-coil electrode tension spring. Four of these springs were attached to the copper bus at the free end of each heater stage, as shown in figure 5. Thus, on each heater stage, the springs were mechanically in parallel. Figure 10 is a curve of the force-deflection behavior of one of the springs. The electrode tension spring force is linear over the deflection-region of interest, and the spring constant is the slope of the force-deflection curve. As shown in figure 10, the spring constant is about 115 pounds per inch (201 N/cm) of deflection. Or for four springs mechanically in parallel, the spring constant is 460 pounds per inch (804 N/cm).

Refer to run 3 in table I as an example of the purpose of the electrode tension spring for which the average surface temperature of the fourth heater stage is 4400<sup>o</sup> R (2440<sup>o</sup> K). At this temperature, the unrestrained 8-inch (20.3-cm) effective heater length would increase to about 8.1 inches (20.6 cm) based on a  $\Delta T$  of 4000<sup>o</sup> R (2225<sup>o</sup> K) and an average

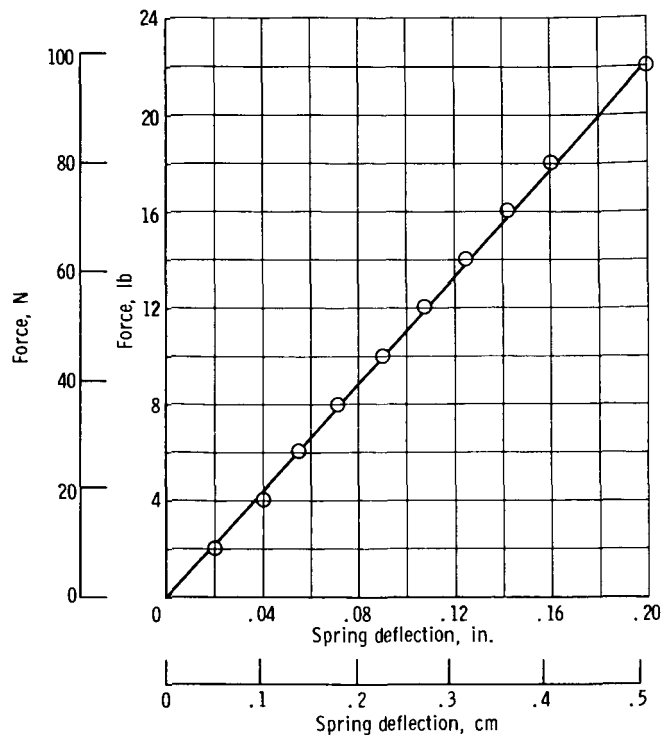
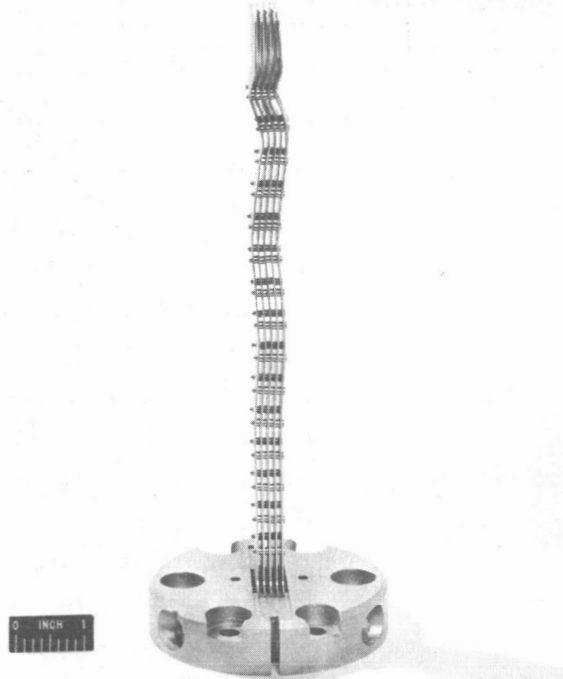


Figure 10. - Force-deflection characteristics of four-turn electrode tension spring. Spring constant, 115 pounds per inch (201 N/cm).

coefficient of linear expansion of  $3 \times 10^{-6}$  inch per inch per  $^{\circ}\text{R}$  ( $5.4 \times 10^{-6}$  cm/(cm)( $^{\circ}\text{K}$ )) as given in reference 8. If however, both ends of the heater plates were restrained, the heater-plate assembly would buckle as a unit and cause flow blockage in the outer passages surrounded by the boron nitride housing. Figure 11 illustrates an example of insufficient tension applied to the heater element.

The predetermined tension force applied to the springs during assembly was about 144 pounds (640 N) which corresponds to an initial deflection in the tension springs of 5/16 inch (0.79 cm). Since the heater-plate cross-sectional area is 0.15 square inch ( $0.97 \text{ cm}^2$ ), the initial room-temperature stress is 960 psi ( $661 \text{ N/cm}^2$ ). At operating temperature, the heater elements expand about 0.1 inch (0.254 cm) thus reducing the tension to about 97 pounds (432 N) corresponding to a stress of 650 psi ( $448 \text{ N/cm}^2$ ). The heater operational goal was set at 10 hours. The heater elongation was calculated to be less than 0.001 inch (0.0025 cm) by using the creep and stress data of reference 9. Test results confirmed that the elements, when placed under the specified initial tension, did not creep more than 0.001 inch (0.0025 cm).

During operation, the heater elements are in the vertical position. Two guide-rods and electrical insulating sleeves are used for alignment to prevent twisting or cocking of



C-65-2007

Figure 11. - Heater-element buckling resulting from insufficient tension in electrode tension springs.

the elements due to uneven spring tension. These guide-rods and sleeves are shown photographically in figure 8.

## Materials of Construction

The heating element and its flow housing are the two components that must operate near  $5000^{\circ}\text{R}$  ( $2780^{\circ}\text{K}$ ) in a flowing hot gas stream. The choice of materials for these components was an important consideration for the successful operation of the heater. The other heater components, such as the water-cooled electrical busing, the containment vessel, and gas flow system, all operate near ambient temperature so that the usual construction materials could be used.

The heating element had to be a refractory material that possessed the following characteristics:

- (1) Electrical resistivity that meets the requirements of a low-voltage, high-current power supply
- (2) Easy machinability into the desired shapes

- (3) Nonreactivity with hydrogen, helium, and nitrogen gases at local surface temperatures up to  $5500^{\circ}$  R ( $3055^{\circ}$  K)
- (4) Operating capability at  $5000^{\circ}$  R ( $2780^{\circ}$  K) for 10 hours without significant dimensional changes

Tungsten was selected as the material that best met these requirements because, of all the refractory metals, it has the highest melting point  $6620^{\circ}$  R ( $3680^{\circ}$  K). Therefore, at an operating temperature of  $5000^{\circ}$  R ( $2780^{\circ}$  K), it will retain more of its original strength than other lower melting point refractory metals such as rhenium or tantalum. Tungsten electrical resistivity is relatively low which makes it compatible with a high-amperage - low-voltage power supply.

The chemical reaction between tungsten and the gases used is insignificant. The only precaution is that the oxygen content of the gas must be sufficiently low to prevent oxidation of the tungsten. The oxygen content of the gases used in these tests was less than 50 parts per million. No apparent oxidation occurred.

In the form of a single, thin, unsupported plate, tungsten will deform at high temperature and load. However, with adequate supports, as shown in figure 4, the heater element will maintain its shape at  $5000^{\circ}$  R ( $2780^{\circ}$  K) under both aerodynamic and electromagnetic forces which result from the flow of gas over the plates and the current through the plates. For example, reference 2 states that steady-state current values of 14 000 amperes produced electromagnetic forces on the outside plates as high as 3 pounds per inch ( $5.26$  N/cm) of plate length.

During the heater development, tungsten fabrication techniques were improved to simplify some of the more difficult machining operations. As an example, figure 4 shows a side view of a section of the heater assembly. Coiled tungsten serves as nuts. The bolt is unique in that it consists of a tungsten rod over which a tightly wound tungsten coil forms the thread. These coiled bolts and nuts are commercially available and were incorporated into the design. The previously used conventional type of machined tungsten bolt and a sheet metal tungsten nut are also shown in figure 4.

The operating life of a spacer-supported heater is primarily a function of the diffusion rate for tungsten at  $5000^{\circ}$  R ( $2780^{\circ}$  K) into a flowing gas stream. The diffusion rate for this system was not calculated. An estimate of the maximum loss rate can be determined from the evaporation rate of tungsten in a vacuum. At  $5500^{\circ}$  R ( $3055^{\circ}$  K), this rate of 0.0001 inch per hour (0.000254 cm per hour, ref. 10) for 10-hour operation results in a decrease in heater element thickness of 0.002 inch (0.0051 cm) per plate, or approximately a 7-percent change in cross-sectional area. A change of this magnitude could result in a premature heater burnout. However, the vaporization rates would be less under pressure, and an operating life of 10 hours appears as a reasonable goal when 0.030-inch- (0.076-cm-) thick tungsten heating elements are used. In fact, 10 hours of successful heater operation has been achieved, but because of the nature of the tests, this

period included several shutdowns as well as different flow rates and different gases.

The heater flow housing must also be a refractory material capable of operation at  $5000^{\circ}\text{R}$  ( $2780^{\circ}\text{K}$ ), an electrical insulator, nonreactive with hydrogen, helium, and nitrogen, and machinable into the desired shapes. Boron nitride possessed most of these properties and proved to be an excellent material for this component. An initial problem of excessive cracking and spalling was attributed to moisture being absorbed by the boron nitride at room temperature and being rapidly expelled from the material at high temperature. Fortunately, a moisture-resistant grade of boron nitride became available which eliminated this problem. At high temperatures, direct contact between boron nitride and tungsten produces a chemical reaction. The heater section is designed so that direct contact between boron nitride and tungsten is eliminated.

The entire heater assembly was designed so that components adjacent to the heater elements would have at least equivalent operating life. In addition, component replacement could be made without completely disassembling the entire heater assembly. For example, if one heater stage burns out, it can be replaced without completely disassembling the remaining three stages. Normally, the only components being replaced are the heater elements in the third and fourth stages. The boron nitride flow housing can be reused many times. All the tungsten heater element parts can be procured and stocked prior to a shutdown. To disassemble, rebuild, and reassemble the four heater stages requires about 3 man-days.

### Effect of Heater Dimensions on Operating Conditions

In order to achieve maximum gas temperature, the heater surface must operate at the highest temperature consistent with the structural strength of the materials. The length to diameter ratio of the flow passage must be large enough so that the gas temperature approaches the heater surface temperature. For a given outlet gas temperature and heater configuration, a minimum heater length and pressure drop result when the heater surface is maintained at a constant maximum temperature.

As an example, the equation

$$\frac{l}{D} = \frac{1}{2f} \ln \frac{T_w - T_1}{T_w - T_2}$$

derived in reference 11 and based on Reynolds analogy, can be used to calculate a minimum  $l/D$  of 220 under the following conditions: an average friction factor of 0.005, which is consistent with the mass velocity range anticipated in the heater, a surface

temperature of  $5000^{\circ}\text{R}$  ( $2780^{\circ}\text{K}$ ), a gas outlet temperature of  $4500^{\circ}\text{R}$  ( $2500^{\circ}\text{K}$ ), and a gas inlet temperature of  $500^{\circ}\text{R}$  ( $278^{\circ}\text{K}$ ).

However, unless the heater cross-sectional area is varied, a constant heater surface temperature cannot be achieved under conditions of a constant heat-transfer coefficient and a heater material whose resistance increases with increasing temperature. Varying the heater cross-sectional area is not practical, particularly with a material like tungsten that is brittle at room temperature and difficult to fabricate. Using plates with constant cross-sectional area, however, puts a serious restriction on the heater surface temperature profile. For example, if the heater were fabricated from a single flat plate assembly with an  $l/D$  of 256, the heater surface temperature would increase exponentially along the heater length according to an equation of the form

$$T_W = F + Cl^{-a}El$$

This equation is derived in appendix B, where  $a$ ,  $F$ ,  $C$ , and  $E$  are constants based on flow rate, heater dimensions, specific heat, current, inlet temperature, a constant heat-transfer coefficient, and the relation between the resistivity and temperature of tungsten. A typical exponential heater temperature profile is shown in figure 12. This profile re-

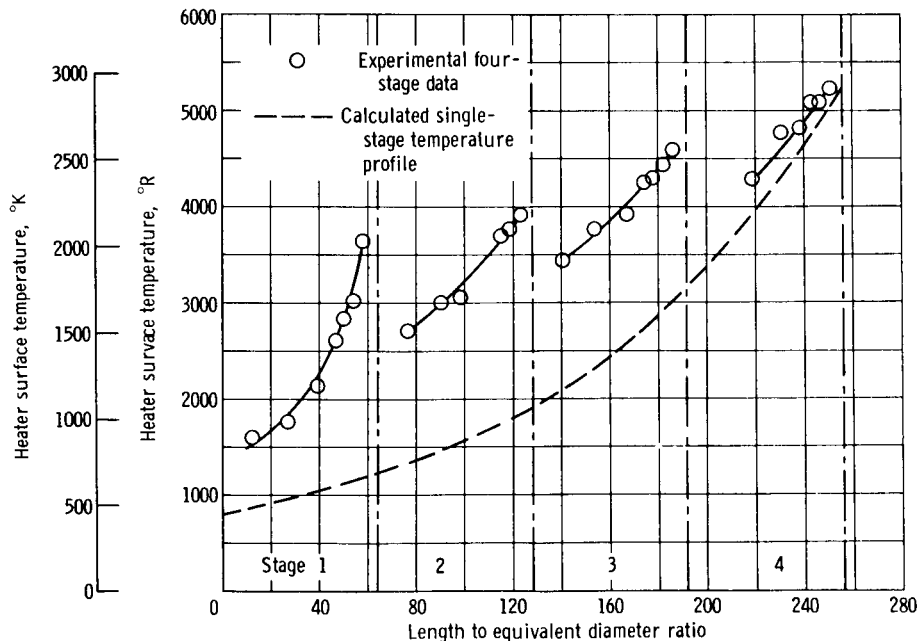


Figure 12. - Comparison between calculated and experimental heater temperature profiles. Calculated profile for single-stage-heater; experimental-temperature data from four-stage heater. Helium flow rate, 0.043 pound per second (19.6 g/sec); maximum surface temperature,  $5240^{\circ}\text{R}$  ( $2910^{\circ}\text{K}$ ); equivalent diameter, 0.0104 feet (0.317 cm); outlet gas temperature: four stage,  $4230^{\circ}\text{R}$  ( $2350^{\circ}\text{K}$ ); single stage,  $3000^{\circ}\text{R}$  ( $1667^{\circ}\text{K}$ ).

sults in an average surface temperature even lower than a linear temperature profile. A heater with this type of temperature profile would be extremely inefficient. In order to achieve a high gas temperature from this low average surface temperature, the  $l/D$  of the heater would have to be increased; thus, the pressure drop would increase accordingly.

An alternate approach (other than varying heater cross-sectional area) to obtain a higher average heater surface temperature would be to divide the heater length into an infinite number of heaters, each with individually controlled power supplies. Four flat-plate heater stages, described in the section Heater Assembly, were chosen as a compromise to approach a higher average heater temperature. Some of the factors that influenced the choosing of four heater stages were

- (1) An  $l/D$  of 256 (which was considered to be large enough to heat the gas) could be obtained by using four identical heaters similar in design to those which had been successfully run and reported in reference 2
- (2) The flexibility and economy associated with four identical heaters and four identical power supplies
- (3) The complexity of additional busing offsets any advantages gained in adding heater stages; conduction losses also increase as more busing is added to accommodate additional stages

Figure 12 shows an actual four-stage heater temperature profile corresponding to run 6 of table I. This profile was obtained by the use of voltage taps connected to the tungsten support bolts along the length of the plates. The surface temperature profile was then obtained from the relation between resistivity and temperature for tungsten, as discussed in the section Method of Calculation. Each heater stage operates at a progressively higher average surface temperature because the gas entering each successive stage is at a higher gas temperature. For a comparison, a calculated temperature profile is also shown in the figure. The calculated temperature profile for the heater stage is not broken up into individual stages supplying different amounts of power. For the same flow rate,  $l/D$ , and maximum surface temperature, the outlet gas temperature is only  $3000^{\circ}\text{R}$  ( $1667^{\circ}\text{K}$ ) compared with  $4230^{\circ}\text{R}$  ( $2350^{\circ}\text{K}$ ) for the four-stage heater. The four-stage heater profiles for the first three stages were not run at the maximum power levels. If they were, each profile would have been at an even higher average surface temperature.

In an attempt to improve the heater performance further, seven 0.020-inch- (0.051-cm-) thick plates spaced 0.040 inch (0.102 cm) apart were substituted for the five 0.030-inch- (0.076-cm-) thick plates. Both sets of plates have approximately the same electrical resistance. As a result, the heat-transfer surface area has been increased about 40 percent and the  $l/D$  about 56 percent. The thinner plates, although capable of withstanding the aerodynamic forces, were not able to support the electromagnetic forces

resulting from the large current flowing through the plates. The 0.020-inch- (0.051-cm-) thick plates buckled even with 1/2 inch (1.27 cm) support spacing.

It is important to realize that a significant pressure drop occurs with a spacer-supported heater even at the low flow rates. Experimental pressure levels between stages are listed in table I. This same pressure drop may also be calculated by a method reported in reference 2. In designing a spacer-supported heater, care should be taken to provide for the additional pressure to overcome the friction pressure drop due to the spacers.

## CONCLUDING REMARKS

A high-temperature four-stage flat-plate gas heater has been designed and is operational. This heater has heated hydrogen, helium, and nitrogen to gas temperatures above  $4500^{\circ}$  R ( $2500^{\circ}$  K). The highest gas temperature,  $4950^{\circ}$  R ( $2750^{\circ}$  K), has been achieved with hydrogen at a mass velocity of 3.0 pounds per square foot per second ( $14.7 \text{ kg}/(\text{m}^2)(\text{sec})$ ). The highest mass velocity, 123.5 pounds per square foot per second ( $604 \text{ kg}/(\text{m}^2)(\text{sec})$ ), was obtained with nitrogen at a gas temperature of  $3700^{\circ}$  R ( $2055^{\circ}$  K). The heater has operated successfully for 10 hours, but this 10-hour period has been achieved with several shutdowns as well as different flow rates and different gases.

The heater design is simple yet offers several unique advantages as follows:

1. The heater is divided into four individually controlled heater stages which allow the heater to operate at a high average surface temperature.

2. The flat-plate heating elements are easy to fabricate. All stages are identical and the parts are interchangeable. Individual components can be replaced without disassembling the entire heater assembly.

3. The flat-plate heating elements can be used with all nonoxidizing gases. The flat plates are uniform in construction and are not as susceptible to hot spotting as are some loosely-woven mesh heaters.

In addition, gas bypass around the heating elements has been minimized by making a positive seal at one end of each heater stage. Thus a higher outlet gas temperature can be obtained for a given maximum surface temperature. Heater expansion is accommodated by water-cooled electrode tension springs. The tension springs also provide busing connections between the tungsten heater elements and rigid power-supply busing.

There are two disadvantages associated with the flat plate heater design:

1. The large friction pressure drop through the spacer-supported plates



2. The voltage drop penalty resulting from small water-cooled buses. (This busing voltage drop reduces the voltage available for the heater itself.)  
Both of the disadvantages are predictable.

Lewis Research Center,  
National Aeronautics and Space Administration,  
Cleveland, Ohio, September 13, 1967,  
(120-27-04-56-22.)

## APPENDIX A

### SYMBOLS

A	current flow cross-sectional area, ft <sup>2</sup> ; m <sup>2</sup>
a	$KI^2\alpha/A_p$ , Btu/(sec)(ft <sup>2</sup> )(°R); J/(sec)(m <sup>2</sup> )(°K)
b	$a\beta/\alpha$ , Btu/(sec)(ft <sup>2</sup> ); J/(sec)(m <sup>2</sup> )
C	constant of integration, °R; °K
$c_p$	specific heat of gas at constant pressure, Btu/(lb)(°R); J/(kg)(°K)
$\bar{c}_{p_g}$	mean specific heat of gas at constant pressure through heat exchanger, Btu/(lb)(°R); J/(kg)(°K)
$c_{p_w}$	specific heat of water at constant pressure, Btu/(lb)(°R); J/(kg)(°K)
D	equivalent diameter, ft; m
E	$hp/Wc_p(a - h)$ , (ft)(sec)(°R)/Btu; (m)(sec)(°K)/J
F	$-b/a$ , °R; °K
f	average friction factor
H	$(-b - hT_i)/(a - h)$ , (ft)(sec)(°R)/Btu; (m)(sec)(°K)/J
h	heat-transfer coefficient, Btu/(sec)(ft <sup>2</sup> )(°R); J/(sec)(m <sup>2</sup> )(°K)
I	current, A
K	conversion factor from watts to Btu/(sec), $0.948 \times 10^{-3}$
l	position along axial length, ft; m
dl	differential length element, ft; m
Δl	incremental length of element, ft; m
P	total perimeter of all plates, ft; m
q	local heat flux from plates to gas, Btu/(sec)(ft <sup>2</sup> ); J/(sec)(m <sup>2</sup> )
$T_b$	bulk gas temperature, °R; °K
$T_i$	inlet gas temperature at $l = 0$ , °R; °K
$T_w$	surface temperature, °R; °K
$T_1$	heater exit gas temperature, °R; °K
$T_2$	heat exchanger outlet gas temperature, °R; °K

$\Delta T_1$	heat exchanger water temperature increase, $^{\circ}\text{R}$ ; $^{\circ}\text{K}$
$V_0$ to $V_6$	voltage locations designated in fig. 5
$\Delta V$	incremental voltage drop, V
W	gas flow rate, lb/sec; kg/sec
$W_1$	water flow rate in heat exchanger, lb/sec; kg/sec
$\alpha$	constant, ohm-ft/ $^{\circ}\text{R}$ ; ohm-cm/ $^{\circ}\text{K}$
$\beta$	constant, ohm-ft; ohm-cm
$\zeta$	resistivity of tungsten, ohm-ft; ohm-cm

## APPENDIX B

### DERIVATION OF WALL TEMPERATURE PROFILE AS FUNCTION OF HEATER LENGTH

At a distance  $l$  along the passage length (see fig. 13),

$$q = h(T_w - T_b) \quad (B1)$$

$$Wc_p(T_b - T_i) = p \int_0^l q \, dl \quad (B2)$$

$$q = \frac{KI^2}{A} \frac{\zeta}{p} \frac{dl}{dl} = \frac{KI^2 \zeta}{Ap} \quad (B3)$$

where the surface temperature  $T_w$ , bulk temperature  $T_b$ , resistivity  $\zeta$ , and heat flux  $q$  are taken at axial position  $l$ , and the inlet temperature,  $T_i$ , is taken at  $l = 0$ .

The assumptions for wall temperature profile of electrically heated plates are as follows:

- (1) The resistivity of the elements  $\zeta$  is a function of heater wall temperature and varies according to  $\zeta = \alpha T_w + \beta$ , where  $\alpha$  and  $\beta$  are constants.
- (2) The heat-transfer coefficient  $h$  is a constant along the axial length.
- (3) The specific heat  $c_p$  is a constant along the axial length.

Equation (B2) can be expressed in terms of  $T_b$  and substituted into equation (B1) giving

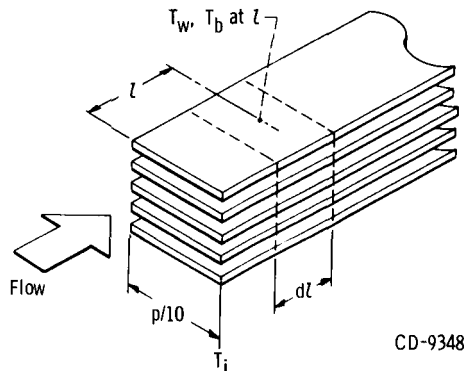


Figure 13. - Schematic of flat-plate configuration used in derivation of wall temperature profile.

$$q = h \left( T_w - \frac{p}{Wc_p} \int_0^l q \, dl - T_i \right) \quad (B4)$$

Since  $\xi = \alpha T_w + \beta$ , equation (B3) can be written as

$$q = \frac{KI^2}{Ap} (\alpha T_w + \beta) \quad (B5)$$

Letting  $a = KI^2\alpha/Ap$  and  $b = a\beta/\alpha$  and substituting into equation (B5) give

$$q = aT_w + b \quad (B6)$$

Equating equations (B4) and (B6) and expressing in terms of  $T_w$  give

$$T_w = \frac{-b - hT_i}{a - h} - \frac{hp}{(a - h)Wc_p} \int_0^l q \, dl \quad (B7)$$

Letting  $H = (-b - hT_i)/(a - h)$  and  $E = hp/(a - h)(Wc_p)$  and using equation (B6) yield equation (B7) in the form

$$T_w = H - E \int_0^l q \, dl = H - E \int_0^l (aT_w + b)dl \quad (B8)$$

Equation (B8) can now be differentiated and expressed as

$$\frac{dT_w}{dl} + EaT_w = -Eb \quad (B9)$$

Equation (B9) is a linear first-order differential equation the solution of which yields

$$T_w = -\frac{b}{a} + Ce^{-aEl} = F + Ce^{-aEl} \quad (B10)$$

where the constant  $C$  can be evaluated from the boundary conditions: at  $l = 2.67$  feet (0.814 m),  $T_w = 5240^\circ \text{R}$  ( $2910^\circ \text{K}$ ), and  $F = -b/a$ . Equation (B10) was used to calculate the wall temperature profile of figure 12 with a helium flow rate of 0.043 pound per

second (19.6 g/sec) corresponding to run 6 in table I. In addition, the maximum wall temperature of the calculated profile was limited to  $5240^{\circ}\text{R}$  ( $2910^{\circ}\text{K}$ ), the maximum wall temperature of run 6. The other parameters used to calculate the wall temperature profile are as follows:

Gas flow rate (of helium), $W$ , lb/sec; g/sec . . . . .	0.043; 19.6
Total perimeter of all plates, $p$ , ft; m . . . . .	0.833; 0.254
Specific heat of gas at constant pressure, $c_p$ , Btu/(lb)( $^{\circ}\text{R}$ ); J/(kg)( $^{\circ}\text{K}$ ) . . . . .	1.25; $5.23 \times 10^3$
Current flow cross-sectional area, $A$ , $\text{ft}^2$ ; $\text{cm}^2$ . . . . .	$1.042 \times 10^{-3}$ ; 0.968
Heat-transfer coefficient, $h$ , Btu/( $\text{ft}^2$ )(sec)( $^{\circ}\text{R}$ ); J/(sec)( $\text{m}^2$ )( $^{\circ}\text{K}$ ) . . . . .	0.07; $14.3 \times 10^2$
Inlet gas temperature at $l = 0$ , $T_i$ , $^{\circ}\text{R}$ ; $^{\circ}\text{K}$ . . . . .	560; 311
Position along axial length, $l$ , ft; m . . . . .	2.67; 0.814
Equivalent diameter, $D$ , ft; cm . . . . .	0.0104; 0.317
Current, $I$ , A . . . . .	6900
Constant of integration, $C$ , $^{\circ}\text{R}$ ; $^{\circ}\text{K}$ . . . . .	565; 314
Constant, $\alpha$ , ( $\mu\text{ohm}$ )(ft)/ $^{\circ}\text{R}$ ; ( $\mu\text{ohm}$ )(m)/ $^{\circ}\text{K}$ . . . . .	$0.583 \times 10^{-3}$ ; $0.32 \times 10^{-3}$
Constant, $\beta$ , ( $\mu\text{ohm}$ )(ft); ( $\mu\text{ohm}$ )(m) . . . . .	-0.146; -0.0445

In this investigation, the values of  $\alpha$  and  $\beta$  are used to linearize the temperature-resistivity relation for tungsten given in reference 7.

## REFERENCES

1. Lietzke, Armin F.: Feasibility Study of a Tungsten Water-Moderated Nuclear Rocket. III. Fuel Elements. NASA TM X-1422, estimated publication, approximately Dec. 1967.
2. Slaby, Jack G.; Maag, William L.; and Siegel, Byron L.: Laminar and Turbulent Hydrogen Heat Transfer and Friction Coefficients Over Parallel Plates at 5000<sup>0</sup> R. NASA TN D-2435, 1964.
3. Maag, William L.; and Mattson, William F.: Forced-Convection Heat-Transfer Correlations For Gases Flowing Through Wire Matrices at Surfaces Temperatures to 5500<sup>0</sup> R. NASA TN D-3956, 1967.
4. Anon.: Thermocouples and Thermocouple Extension Wires. Rev. Composite of RPI.9-RPI.7, Instr. Soc. Am., July 1959.
5. Grier, Norman T.: Calculation of Transport Properties and Heat-Transfer Parameters of Dissociating Hydrogen. NASA TN D-1406, 1962.
6. Hilsenrath, Joseph, et al.: Tables of Thermal Properties of Gases. Circular 564, National Bureau of Standards, Nov. 1, 1955.
7. Weast, Robert C., ed.: Handbook of Chemistry and Physics. 37th ed., Chemical Rubber Publishing Co., 1955, p. 2360.
8. Schmidt, F. S.; and Ogden, H. R.: The Engineering Properties of Tungsten and Tungsten Alloys. DMIC Rep. No. 191, Battelle Memorial Inst., Sept. 27, 1963.
9. Green, Walter V.: Short-Time Creep-Rupture Behavior of Tungsten at 2250<sup>0</sup> to 2800<sup>0</sup> C. Trans. AIME, vol. 215, no. 6, Dec. 1959, pp. 1057-1060.
10. Rom, Frank E.: Fast and Moderated Low-Power, Lightweight Reactors for Nuclear Rocket Propulsion. Paper presented at the Second Lecture Series on Nuclear and Electric Rocket Propulsion, AGARD, Brussels, Belgium, Sept. 28-Oct. 3, 1964.
11. Knudsen, James G.; and Katz, Donald L.: Fluid Dynamics and Heat Transfer. McGraw-Hill Book Co., Inc., 1958.

TABLE I. - OPERATING CONDITIONS FOR SEVEN TYPICAL RUNS

[Run time, approximately 10 min.]

(a) U. S. Customary Units

Operating conditions	Run						
	1	2	3	4	5	6	7
	Test gas						
	Hydrogen		Nitrogen			Helium	
Heater inlet gas temperature, $T_i$ , °R	545	500	520	500	540	560	530
Heater outlet gas temperature, $T_1$ , °R	3680	4240	<sup>a</sup> 4950	3700	4870	4230	4800
Mass velocity, lb/(sec)(ft <sup>2</sup> )	12.7	6.8	3.0	123.5	49.3	17.7	14.8
Gas flow rate, W, lb/sec	0.031	0.0165	0.0073	0.300	0.120	0.043	0.035
Heat exchanger water flow rate, $W_1$ , lb/sec	5.82	5.82	5.82	5.82	5.82	8.34	5.82
Heat exchanger water temperature rise, $\Delta T$ , °R	64.2	41.3	21.7	43.8	24.6	23.6	32.1
Heat exchanger outlet gas temperature, $T_2$ , °R	550	520	525	700	625	560	565
Average surface temperature, °R:							
Stage 1	1290	2010	2360	2390	2180	2165	2300
Stage 2	2500	3085	3165	3080	3230	3055	3245
Stage 3	3355	3770	3970	3860	4225	3785	4035
Stage 4	3900	4060	4400	4110	4725	4430	4750
Voltage drop, V:							
Stage 1	5.40	7.05	6.16	9.50	5.4	7.70	6.70
Stage 2	11.06	9.10	6.50	8.96	8.04	8.95	8.00
Stage 3	15.17	15.20	12.00	14.07	11.0	11.40	12.90
Stage 4	16.60	10.81	10.30	12.00	11.5	12.95	12.06
Current, A:							
Stage 1	$14.5 \times 10^3$	$11.1 \times 10^3$	$8.0 \times 10^3$	$12.2 \times 10^3$	$7.8 \times 10^3$	$11.2 \times 10^3$	$9.1 \times 10^3$
Stage 2	$13.6 \times 10^3$	$8.7 \times 10^3$	$6.0 \times 10^3$	$8.6 \times 10^3$	$7.25 \times 10^3$	$8.6 \times 10^3$	$7.2 \times 10^3$
Stage 3	$13.1 \times 10^3$	$11.4 \times 10^3$	$8.4 \times 10^3$	$10.2 \times 10^3$	$7.2 \times 10^3$	$8.5 \times 10^3$	$8.9 \times 10^3$
Stage 4	$11.9 \times 10^3$	$7.4 \times 10^3$	$6.3 \times 10^3$	$8.1 \times 10^3$	$6.6 \times 10^3$	$8.0 \times 10^3$	$6.9 \times 10^3$
Inlet pressure at stage 1, psia	130	75	50	(b)	(b)	133	152
Outlet pressure, psia:							
Stage 1	129	72	49			125	150
Stage 2	120	60	41			111	145
Stage 3	95	50	35			85	115
Stage 4	59	21	18			45	52

<sup>a</sup>Iridium plug melted at 4910° R.

<sup>b</sup>Pressures not recorded.



TABLE I. - Concluded. OPERATING CONDITIONS FOR SEVEN

TYPICAL RUNS

[Run time, approximately 10 min.]

(b) SI Units

Operating conditions	Run						
	1	2	3	4	5	6	7
	Test gas						
	Hydrogen		Nitrogen		Helium		
Heater inlet gas temperature, $T_i$ , °K	306	278	289	278	300	311	294
Heater outlet gas temperature, $T_1$ , °K	2010	2360	<sup>c</sup> 2750	2060	2705	2350	2670
Mass velocity, kg/(sec)(m <sup>2</sup> )	61.8	33.1	14.6	602	239.5	86.2	72.0
Gas flow rate, W, g/sec	14.1	7.48	3.32	136	54.6	19.6	15.9
Heat exchanger water flow rate, $W_1$ , kg/sec	2.64	2.64	2.64	2.64	2.64	3.79	2.64
Heat exchanger water temperature rise, $\Delta T$ , °K	35.6	23	12.05	24.3	13.6	13.1	17.8
Heat exchanger outlet gas temperature, $T_2$ , °K	305	289	292	389	347	311	314
Average surface temperature, °K:							
Stage 1	716	1115	1310	1325	1210	1205	1280
Stage 2	1390	1710	1765	1710	1795	1695	1802
Stage 3	1865	2090	2210	2140	2370	2100	2240
Stage 4	2160	2255	2440	2280	2620	2460	2640
Inlet pressure at stage 1, N/cm <sup>2</sup>	89.5	51.6	34.4	(b)	(b)	91.6	104.6
Outlet pressure, N/cm <sup>2</sup>							
Stage 1	88.8	49.6	33.7	↓	↓	86	103.3
Stage 2	82.6	41.3	28.2	↓	↓	76.4	99.8
Stage 3	65.4	34.4	24.1	↓	↓	58.5	79.2
Stage 4	40.6	14.5	12.4	↓	↓	31	35.8

<sup>b</sup>Pressures not recorded.

<sup>c</sup>Iridium plug melted at 2730° K.

*"The aeronautical and space activities of the United States shall be conducted so as to contribute . . . to the expansion of human knowledge of phenomena in the atmosphere and space. The Administration shall provide for the widest practicable and appropriate dissemination of information concerning its activities and the results thereof."*

—NATIONAL AERONAUTICS AND SPACE ACT OF 1958

## NASA SCIENTIFIC AND TECHNICAL PUBLICATIONS

**TECHNICAL REPORTS:** Scientific and technical information considered important, complete, and a lasting contribution to existing knowledge.

**TECHNICAL NOTES:** Information less broad in scope but nevertheless of importance as a contribution to existing knowledge.

**TECHNICAL MEMORANDUMS:** Information receiving limited distribution because of preliminary data, security classification, or other reasons.

**CONTRACTOR REPORTS:** Scientific and technical information generated under a NASA contract or grant and considered an important contribution to existing knowledge.

**TECHNICAL TRANSLATIONS:** Information published in a foreign language considered to merit NASA distribution in English.

**SPECIAL PUBLICATIONS:** Information derived from or of value to NASA activities. Publications include conference proceedings, monographs, data compilations, handbooks, sourcebooks, and special bibliographies.

**TECHNOLOGY UTILIZATION PUBLICATIONS:** Information on technology used by NASA that may be of particular interest in commercial and other non-aerospace applications. Publications include Tech Briefs, Technology Utilization Reports and Notes, and Technology Surveys.

*Details on the availability of these publications may be obtained from:*

SCIENTIFIC AND TECHNICAL INFORMATION DIVISION  
NATIONAL AERONAUTICS AND SPACE ADMINISTRATION

Washington, D.C. 20546